

CFRP Prestressed Concrete Lighting Columns

Giovanni P. Terrasi and Janet M. Lees

Synopsis:

Aspects of the design and installation of a novel carbon fibre reinforced polymer (CFRP) prestressed high strength concrete lighting column (Carbolith®) are presented. The tapered cylindrical columns have a nominal height of 8 m and contain an opening above the foundation to allow for the insertion of the lamp fuse box. The bending/torsion behaviour of a total of five full-scale prototype columns was tested in accordance with the relevant European standards (EN). In the experimental programme, the location of the fuse box opening relative to the loading direction was varied. All five poles fulfilled the EN serviceability and ultimate limit state requirements for lighting columns in pedestrian and/or low speed lightly trafficked areas. This successful outcome has led to the first field application of the CFRP prestressed concrete lighting columns.

Keywords: carbon fibre reinforced polymer tendons, prestressing, high strength concrete, lighting columns

Giovanni Terrasi received his PhD from ETH Zürich in 1997. He is currently the head of the R&D/Engineering Department at SACAC AG in Lenzburg, Switzerland and has a particular interest in the behaviour of high performance concrete reinforced or prestressed with fibre reinforced polymer tendons.

Janet Lees received her PhD from the University of Cambridge in 1997. Since 1998, she has been working as a University Lecturer in Structural Engineering at the University of Cambridge, UK. Her research interests include the use of advanced composites in concrete applications and joining techniques for all-composite structures.

INTRODUCTION

In September 2000, the world's first carbon fibre reinforced polymer (CFRP) prestressed high strength concrete electricity pylon was installed in Switzerland⁽¹⁾. The 27 m high pole was manufactured using a centrifugally-cast high strength concrete containing blended silica-fume cement (see Figure 1).

Building on this successful application of CFRP tendons, the potential of transferring the technology to lighting columns was identified. In particular, road environments are known to be very aggressive, causing corrosion at the fixture of plain steel, steel-reinforced or steel-prestressed concrete lighting posts. It is thus a promising application for a structure that combines concrete with a non-corrodible, lightweight and high strength tendon material such as CFRP.

The durability of the CFRP prestressing material is a key advantage in the construction of slender prestressed concrete cylindrical poles. Steel corrodes and, in many applications, a significant concrete cover (40-50 mm) is required to protect the prestressing steel from aggressive internal and/or external environments. In contrast, when durable CFRP tendons are used, only a relatively small concrete cover (15-20 mm) is required. Therefore, CFRP-prestressed poles are significantly lighter than equivalent steel-prestressed structures resulting in lower transportation and installation costs. An additional advantage is that the non-metallic tendons are expected to have low maintenance requirements.

The focus of this project was the design and installation of an 8 m nominal height CFRP prestressed concrete lighting column fulfilling the requirements of the relevant European Standard EN40 Series⁽²⁾⁽³⁾⁽⁴⁾⁽⁵⁾. A particular design consideration was the requirement of an opening above the pole's foundation for the electrical fuse box of the lamp.

In the following, the installation of a prototype Carbolith® CFRP prestressed lighting column is detailed and aspects of the experiments undertaken to confirm the performance of full-scale specimens are discussed.

RESEARCH SIGNIFICANCE

The research investigates the performance of CFRP prestressed high strength concrete lighting columns. The work gives insight into the behaviour of this novel combination of materials when used in a practical application where conventional steel and steel-concrete solutions are known to have limitations in terms of their long-term durability performance.

By carrying out experiments on full-scale columns, in accordance with relevant standards, the system behaviour was verified and a prototype CFRP prestressed lighting column has now been installed in Switzerland. It is expected that the use of non-metallic materials will play an important role in the provision of sustainable infrastructure.

FIELD APPLICATION

In March 2003, an 8 m high prototype Carbolith® lighting column was erected in the SACAC AG car park in Lenzburg, Switzerland (see Figure 2).

The tapered high strength concrete pole was prestressed with six CFRP tendons (prestressed to 60% of the ultimate tendon stress, f_u) and contained no shear reinforcement. It was thus directly comparable to two of the prototype poles tested in the experimental programme that will be described later in this paper. A 1.2 m deep hole was dug and the pole was lifted into place using a light crane. A 0.4 m × 0.4 m × 1.2 m long concrete block was then cast at the foot of the 9.2 m pole (resulting in a final height of 8 m) and acted as the foundation. The pole weight was only 350 kg which represents 70% of the weight of a conventional steel reinforced concrete lighting pole with the same nominal height. The ground was then compacted around the foundation block and additional mortar used to secure the pole in position.

The total material, production and installation costs were equal to that of an equivalent steel-prestressed concrete pole. Thus the poles are expected to be a competitive alternative for lighting in pedestrian and lightly trafficked areas. Further work on the performance under vehicle impact will investigate the suitability for use adjacent to higher speed traffic.

A production line for the 8 m centrifugally-cast CFRP prestressed lighting columns is now being established. In addition, there is a demand for shorter 3.7 m high poles (4.2m total length) for the lighting of residential and pedestrian boardwalk areas. CFRP prestressed concrete poles are currently being developed for this application and incorporate similar technology to that used in the 8 m poles with the exception that they contain only four CFRP tendons and PVA shear reinforcement. Work in this area has been focusing on the optimisation of the production parameters e.g. spinning speed, concrete viscosity, concrete colour, fuse box details, and the installation of the internal shear reinforcement.

These poles cost the same as conventional steel-concrete products. SACAC plans to deliver twenty of the 3.7 m poles by the third quarter of 2003, with a target delivery of fifty poles by the end of 2003. Orders have already been taken from two cities in North-Eastern Switzerland which suggests there is an emerging market for CFRP prestressed concrete lighting columns.

LIGHTING COLUMN DETAILS

The basic configuration and dimensions of the prototype 9.2 m (8 m nominal height) tapered cylindrical lighting columns (henceforth referred to as 'poles') are shown in Figure 3. A Quadralux-G lantern type was assumed since this is one of the most common luminaries for street lighting columns in Europe. The position of the fuse box opening, at 1500 mm from the end of the fixture, and the opening geometry (height = 300 mm, width = 75 mm) were chosen to reflect typical fuse boxes used in central Europe. The pole taper of 10 mm/m results in a variation of the outer diameter from 120 mm at the tip to 212 mm at the foot, the average wall thickness of the pole being 40 mm \pm 10 mm (measured at the tip and foot surfaces).

To confirm the in-service performance of the poles, an extensive experimental programme was devised, in accordance with the relevant EN standards. In total, five CFRP prestressed concrete lighting columns were to be tested. The geometry, concrete and tendon strengths could be considered to be similar for all the specimens (only slight variations were noted). The main differences were the pole internal shear reinforcement and the location of the fuse box during testing.

The poles were centrally prestressed with six CFRP tendons of diameter 4 mm (the tendon material properties are shown in Table 1). The tendons were pultruded rods and had a ceramic coating on the outer surface to improve the bond properties. The initial prestressing force of each CFRP tendon was 16.6 kN ($\sigma_{p0} = 1'320 \text{ N/mm}^2$) corresponding to a total central prestressing force in the pole of 100 kN (at prestress transfer). It is of note that due to the requirement of a fuse box, the tendons were deviated in this region. The opening was defined and reinforced by a stainless steel casing consisting of two deflector-beams to deviate the two tendons running through the fuse box region (see Figure 3).

Three different types of shear reinforcement were adopted for pole numbers 3, 4 and 5 (there was no shear reinforcement in poles 1 and 2). In pole 3, a PVA geogrid (180 kN/m-transverse, 180 kN/m-longitudinal, 90/0°) was used and in pole 4, an aramid-fibre geogrid (150 kN/m-transverse, 30 kN/m-longitudinal, 90/0°) was incorporated. In both cases, the geogrids (used typically for slope stabilisation) had a mesh size of 30 mm, and were wound and fixed over the prestressing reinforcement over a length of either 3.8 m (pole 3) or 5 m (pole 4) from the pole foot. The shear reinforcement of pole 5 consisted of rolltruded CFRP tapes of cross section 2 \times 0.14 mm \times 13 mm, with an average tensile strength of 2'500 N/mm² and a Young's Modulus of about 150'000 N/mm². The

CFRP tapes were spirally wound around the longitudinal tendons with a pitch of 35 mm.

The high strength concrete (HSSC) corresponded to strength class B100/90 (550 kg rapid hardening cement CEM II/A-D 52.5, 8% silica-fume, 0-6 mm aggregates, w/c = 0.3). Typical mechanical properties of the mix were; a minimum 28 day compressive cube strength of over 90 MPa, a minimum tensile strength of 5 MPa, a Young's Modulus of 38,550 MPa, an ultimate strain of 0.0035 and a shear strength of 0.83 MPa. The concrete was compacted using a centrifugal casting process in a pretensioning/spinning mould made of steel. Prestress transfer occurred 36-42 h after the centrifugation process.

Two weeks after production, a reinforced concrete foundation block with dimensions 360 × 360 × 1200 mm was cast over the foot region of each of the five pole specimens (see Figure 3) resulting in a 1.2 m fixture length for the planned cantilever tests (this length represents a medium fixture length for an 8 m nominal height pole as specified in EN40-2⁽³⁾).

SPECIMEN DESIGN

Applied Loads

The most relevant loading condition for the lighting columns was the wind. A terrain category II (which is for flat areas with occasional small structures) and a basic wind velocity at 10 m above sea level (30 m/s) were assumed. Using a mean shape factor of 0.52, the resulting average unfactored wind pressure on the pole was 600 N/m². Based on the manufacturer's data, the side-wind pressure surface area of the lantern was 0.14 m² and the front wind pressure surface area was 0.1 m². Using a shape coefficient of 1.0, the resulting unfactored wind pressure on the lantern was calculated in accordance to EN 40-3-1⁽⁴⁾ to be 1'325 N/m².

A partial wind load factor of $\gamma_f = 1.4$ (for transient wind gust action) was used⁽⁴⁾ and the partial load factor for the self-weight was taken to be $\gamma_G = 1.2$.

Wind pressure acting on a cantilevered pole will result in flexural moments relative to any given longitudinal axes. Furthermore, because of the lantern eccentricity, when the wind blows on the side of the lantern, the pole will be subjected to an additional torsional moment. Therefore, the experimental programme included an investigation of both the pure torsion and the bending/torsion response of the poles.

Design Philosophy

The pole was designed to be fully prestressed at maximum service load in order to limit deflections: The formation of bending cracks is to be avoided so that the

moment of inertia of the entire cross section is available to sustain the service moment. The horizontal service deflections of the pole were determined by considering the unfactored ($\gamma = 1.0$) characteristic design loads (self-weight and wind⁽⁴⁾). In the pre-cracked stage the centrally prestressed pole behaved as an elastic tapered cantilever beam (of 8 m free length). The tip deflection under wind load (service load) was limited to a calculated value of 20 mm.

The ultimate bending moments of resistance were predicted using an inelastic analysis based on the short-term stress/strain curves of CFRP and high strength spun concrete. The characteristic material strengths were reduced by appropriate partial material safety factors (1.15 for the CFRP tendons and 1.3 for the dense spun concrete). As in classical prestressed concrete analysis, the equilibrium of internal forces and moments was considered assuming perfect bond and the principle of plane sections remaining plane. Since the section geometry and concrete prestress varied along the length, each pole cross-section was considered separately. The combined interaction of X-X flexural moments (where the fuse box was on either the compressive or tensile face), Y-Y flexural moments (fuse box on the neutral axis) and torsional moments was taken into account.

STATIC TESTS

The experimental programme included freeze-thaw durability, torsion, static bending/torsion and dynamic tests. However, this paper will report primarily on the torsion and static bending/torsion results.

General Arrangement

The five prototype specimens (poles 1-5) were tested in Cambridge, UK. Each pole was fixed to the strong floor by prestressing the end foundation block (over the fixture length of 1200 mm) using three spreader beams and threaded tensioning bars (see Figure 4). The total pressure on the foundation block was 45 tonnes.

In order to test in uni-axial horizontal bending (combined with torsion), all the pole specimens were centrally supported to 'compensate' for the self-weight moment in the vertical plane. The vertical support was located at 3.2 m from the pole tip and consisted of a trolley with wheels that was capable of following the pole deflection. A serial load cell was integrated into the purpose-built trolley support to monitor the reaction force. The off-axis tensile load was introduced at the tip of the pole by means of a specially manufactured steel clamping rig.

Torsion Tests

To verify the integrity of the torsion clamping system and to investigate the torsion-only behaviour of the pole, a test was carried out on pole 1 where a tubular steel bar (of mass 4.2 kg) was welded to the clamping device fixed at the pole tip, giving an effective torsion lever arm of 2.0 m. The torsion load was introduced incrementally by adding standard 2-kg weights on a pan hanging on the end of the steel bar (to a maximum total torque of 280 Nm). For every load step, the corresponding torsion angular displacement was determined by reading an inclinometer bonded on the pole at 65 mm from the tip. The resulting vertical bending moment was negligible because of the limited vertical testing load (with a maximum value of 12 kg) acting on the pole.

Bending/Torsion Tests

In the main bending/torsion cantilever tests, the fuse box opening was positioned on the compression edge for poles 1 and 3 (M_{+x}), along the neutral axis for pole 2 (M_y) and on the tension edge for poles 4 and 5 (M_{-x}) (see Table 2).

The poles had an effective bending lever arm of 7.99 m and a torsion lever arm of 0.14 m (the load eccentricity was imposed using the clamping rig). The clamping rig at the pole tip was pulled horizontally using a threaded rod (with a pitch of 1.5 mm/rotation) connected to a 125 W electric motor, that transferred its rotation onto a M10 nut via a chain-gear (see Figure 4). The electric motor was driven by a potentiometer, from where the rotation (loading) speed and the loading direction could be controlled by the testing engineer. The pulling load was measured and controlled by a tension load cell which was connected via a logger to a data monitoring PC.

Linear Resistance Displacements Transducers (LRDTs) with measuring range 25 mm, 150 mm or 1500 mm were used to monitor the deflection of a pole during testing. Additional displacement transducers were installed to identify any tendon pull-in or any unexpected rotation of the foundation block. The locations of the LRDTs are indicated in Figure 5. The measurement accuracy of all the load cells and displacement transducers complied with the limits specified in the European Standards.

The torsion angular displacement was the only data measured by hand using a spirit level inclinometer bonded over the tip of the pole (mid-point at $x = 7.935$ m from the fixture). The measurement of the crack pattern (crack widths, lengths and positions) was carried out at a reference test load of 1.2 kN by means of a crack magnifying glass and a crack meter.

The serviceability and structural test loads for each verification test were determined by considering the characteristic lantern dead load and wind loads⁽⁴⁾. The serviceability test loads were calculated using the unfactored characteristic wind pressures ($\gamma_f = 1.0$) for the pole shaft and lantern under consideration. By

multiplying the serviceability test loads by the factor $\gamma_u = 1.7$, the minimum ultimate test loads required by the EN⁽⁴⁾ were obtained (see Table 2). The testing regime consisted of applying the load in steps of 0.1 kN up to the serviceability test load, unloading in steps of 0.1 kN back to 0 kN, reloading up to the minimum ultimate test load (again in steps of 0.1 kN), unloading to 0 kN and finally, loading until final failure.

RESULTS AND DISCUSSION

Torsion

No torsion cracks were visible over the load range considered in the torsion-only tests and, accordingly, the experimental torsion moment vs. angle relationship was linear within the measurement precision (0.005°) of the inclinometer used.

In Figure 6, the measured response of pole 1 is compared with the predicted linear elastic pure torsion behaviour of a vertical, 10 mm/m tapered cantilever pure concrete beam (uncracked high strength concrete) with round cross section, outer diameter of 200 mm at fixture and constant wall thickness of 40 mm loaded with an eccentric point load. The fuse box opening and stainless steel casing were not taken into account in the calculation model.

The measured torsion angle of 0.135° at the maximum test load ($T = 276.6 \text{ Nm}$) is 12.7% lower than the calculated value of 0.155° . The slightly higher experimental stiffness can be attributed in part to a higher effective shear modulus for the pole than the assumed average value of $G = 16.4 \times 10^9 \text{ N/m}^2$ computed using a Poisson's ratio of $\nu = 0.175$ and an average Young's modulus of concrete $E_{co} = 38'550 \text{ N/mm}^2$ (at low stresses E_{co} is higher than the average value). Differences in wall thickness t (the taper of the production mould results in $t > 40 \text{ mm}$ in the pole foot region and $t < 40 \text{ mm}$ in the pole tip region) may also play a role.

No slippage was observed in the clamping rig designed to apply the torsion load to the pole, which confirmed that the rig was suitable for use in the subsequent cantilever bending/torsion tests.

Static Bending/Torsion

The main results of the bending/torsion cantilever tests of poles 1 – 5 are shown in tables 2 and 3.

The experimental cracking loads (between 0.80 and 1.0 kN) were above the serviceability test loads calculated for the poles according to EN 40-3-1⁽⁴⁾ (where $F_{ser}^{x-x} = 0.56 \text{ kN}$, $F_{ser}^y = 0.506 \text{ kN}$). The poles could therefore be confidently considered to be fully prestressed under serviceability conditions. Furthermore, there was ample reserve load capacity after cracking so the appearance of cracks

would provide a warning, well before imminent failure, that the structure had been subjected to load levels higher than anticipated.

The un-loading of the poles from the service test load gave rise to very low residual deflections, in the range of 1-3 mm. These values were significantly lower than the EN-40-3-2 allowable limits which correspond to residual deflections of between 8.5 and 10.36 mm depending on the particular pole considered (the code states that the residual deflection after removal of the service test load should be less than 20% of the deflection caused by the test load).

Standard EN40-3-2⁽⁴⁾ clause 5.2 b defines an additional serviceability requirement for lighting columns where the temporary horizontal tip deflection corresponding to the minimum serviceability test load shall not exceed 4% of the nominal height of the column for class I acceptance (highest stiffness requirement for lighting columns). The experimental deflections at the service test load were between 42 and 52 mm (see Table 2) indicating that the EN requirement ($\delta_{tip} < 320$ mm) was easily satisfied by all the poles.

All the poles cracked at a load greater than the predicted design cracking load of 0.6 kN (at the lower edge of the fuse box opening for M_x (poles 4,5) and M_{+x} (poles 1,3)) and 0.79 kN (at fixture for M_y – pole 2) which suggests that either the actual concrete tensile strength was higher than expected and/or the prestress force was higher than anticipated. If a prestress loss of 16.7% due to elastic pole shortening, shrinkage and creep of the high strength spun concrete⁽⁵⁾ and a mean wall thickness of 40 mm are assumed, then based on the experimental cracking loads and the position of the first crack, the mean experimental tensile strength in bending of the HSSC was back-calculated to be 6.1 N/mm². This value is slightly higher than the assumed design strength of 5 N/mm².

The deflections started to increase rapidly after cracking of the pole occurred and the rotations concentrated in many thin and well distributed cracks near the fixture and the opening region of the pole. A crack mapping in the tensile region of each pole was carried out at a reference load of 1.2 kN. The fairly good bond between the ceramic coated tendons and the concrete matrix led to the formation of between 4 and 10 thin vertical bending cracks (of widths 0.01 - 0.20 mm) at regular spacings near the fixture and opening regions of the pole (see Figure 7). All the observed cracks were vertical bending cracks and had a maximum width of about 0.5 mm.

When un-loading the specimens from the EN minimum ultimate test load (cracked stage), the bending cracks closed (most of them were no longer visible) and consequently the deflections recovered almost completely (almost perfect elastic behaviour). Therefore only a modest amount of energy dissipation took place during the loading/un-loading cycle.

The deflected bending shapes of pole 3 at various stages of loading are shown in Figure 8. Large deflections were noted in the later stages of testing and the tip deflection was around 925 mm immediately prior to failure. The high rotation capacity came from the opening of the aforementioned thin bending cracks,

originating from the fixture/opening area. Figure 9 shows a photo of the large deflections experienced by pole 3 just before failure: A high deformation capacity in the cracked state could therefore be achieved, despite the use of two brittle material components (CFRP, HSSC). This can be interpreted as a further warning by the system of impending failure when loaded to unforeseen high levels.

The pole failure loads (between 1.56 and 1.89 kN) were considerably higher than the EN minimum required ultimate loads of $F_u^{\min,x,-x} = 0.95$ kN, $F_u^{\min,y} = 0.86$ kN⁽⁴⁾ which indicates a factor of safety in excess of the minimum requirement. The experimental failure moments were reasonably close to the predicted design moment capacities, computed under the assumption of pure bending along the plane considered and including material partial safety factors. In Table 3, both the predicted and experimental ultimate moment capacities at selected cross-sections, and the corresponding tip loads (shown in parentheses) are indicated. The fuse box opening location for each of the tests may be found in Table 2.

Several failure modes were observed, depending on the testing position (bending plane considered) and on the reinforcement configuration (see Figure 10). Poles 1 and 2 failed by the sudden snapping of the CFRP tendons on the tensile edge at cross sections near the fixture (the corresponding moments are M_{u+x} (pole 1, $x = 0.28$ m) = 12.6 kNm, M_{uy} (pole 2, $x = 0.05$ m) = 14.2 kNm). However, while the failure for pole 2 was expected to be near the fixture (Figure 10(a)), pole 1 was predicted to fail in the concrete at the lower edge of the fuse box opening, which was not the case, possibly because of the reinforcing effect of the stainless steel casing that was neglected when determining the pole capacities and the inherent material partial safety factors. Pole 3 (with the opening on the compression edge) contained additional longitudinal passive reinforcement in the form of the PVA fibre bundles. This reinforcement acted to increase the tensile capacity of the cracked pole in the area of the opening and at the fixture and shifted the failure from the tensile to the compressive edge. The result was a combined failure with buckling of the steel casing and concrete crushing at a height 1.5 m from fixture (Figure 10(b)). The experimental failure bending moment was 12.3 kNm, which is 23% higher than that calculated for the HSSC crushing at the lower edge of the opening (Table 3). Again, the difference is attributed to the reinforcing effect of the steel casing and material safety factors. Poles 4 and 5 were tested with the box opening at the tensile flange, therefore the bending resistance of the area around the lower opening edge was reduced since the two CFRP tendons running next to the tensile edge were deflected inwards. Consequently, poles 4 and 5 failed by the sudden snapping of the CFRP tendons on the tensile edge at cross sections at $x = 1.23$ m and $x = 1.5$ m from the fixture respectively. The failure loads and failure locations were reasonably close to the predicted values taking into account the offset of the tendons. In general, the design computation models gave fairly good predictions of the ultimate load capacities.

The load vs. deflection behaviour of all 5 poles (see Figure 11) was nearly bilinear, with a high bending stiffness in the uncracked state and then a gradual loss of stiffness after cracking. The calculated bending stiffness for the uncracked state corresponded exactly to the experimental values. However, the design tip deflection at the ultimate load of 1'304 mm, was considerably higher than the measured values which ranged from $\delta_u^{\text{tip}} = 474.8$ mm (pole 4) to 920.8 mm (pole 3). The reasons for this overestimate of the deflection at failure were most likely due to the underestimation of the tensile strength of the HSSC and the neglect of the tension stiffening effect of the concrete between the bending cracks in the original design model.

To give an indication of the significance of these factors, a further deflection calculation was undertaken where a concrete tensile strength of 6.1 MPa was used (which made a small difference to the results) and tension stiffening was incorporated using Branson's formula, modified to take into account the use of FRP tendons (ACI 440 I⁽⁶⁾, equation 4-1) where

$$I_e = \left(\frac{M_{cr}}{M_a} \right)^3 \beta_d I_g + \left(1 - \left(\frac{M_{cr}}{M_a} \right)^3 \right) I_{cr} \leq I_g \quad (1)$$

and

$$\beta_d = 0.5 \left[\frac{E_f}{E_s} + 1 \right] \quad (2)$$

In these equations, E_f and E_s are the modulus of elasticity of the FRP tendon and steel respectively, M_{cr} is the cracking moment and M_a is the maximum moment at the section where the deflection is considered. The pole cross-section tapers along its length, so to simplify the calculation, the ratio of the cracked moment of inertia I_{cr} to the gross moment of inertia I_g was taken to be constant throughout the cracked region. The total tip deflection was then determined by integrating the cracked curvatures $\kappa_c = M/E_c I_e$ (which takes into account tension stiffening) from the fixture to the end of the cracked region (x_{cr}) and then integrating the uncracked curvatures ($\kappa_e = M/E_c I_g$) from x_{cr} to the pole tip. The resulting curve has been plotted in Figure 11 and the analysis shows very good agreement with the experimental deflections.

For the five pole specimens, no slippage (draw-in) of the tendons, even at the maximum load, was recorded by the LRDTs monitoring the tendons' end-surfaces at the end of fixture (Figure 5). Transfer tests on a plate specimen with similar $\varnothing 4$ mm CFRP tendons and a concrete cover of 18 mm suggested that for a prestressing level of 1000 N/mm² the transfer length was only 70 mm ($17 \times \varnothing_{\text{CFRP}}$). Therefore the foundation length of 1.2 m was more than sufficient to anchor the tendons.

The experimental investigation confirmed that both the serviceability and ultimate limit state static bending/torsion performance of the Carbolith® poles fulfilled the EN requirements. As a result, the first field application of this promising technology has now been implemented.

CONCLUSIONS

(1) The full prestressed design of the CFRP prestressed high strength spun concrete lighting column was verified by testing five specimens in accordance with EN-40-3-2⁽⁴⁾. The serviceability, structural and minimum ultimate load requirements were fulfilled by all the pole specimens tested in cantilever bending/torsion.

(2) The poles showed sufficient bending rotation capacity to make up for the lack of plasticity of the brittle CFRP prestressing tendons. This high rotation capacity in the cracked state (in the load range above the maximum service loads) led to the attainment of a high deflection at failure, with a medium amount of well distributed and thin bending cracks, which can be interpreted as a warning of the pending failure of a pole when loaded to an unforeseen high load level.

(3) The static calculation procedures developed for planning and predicting the behaviour of the prototypes were in accordance with the relevant standard EN40 series and proved to be adequate and mostly conservative mathematical tools for the design of the novel lighting columns. The deflections calculated using the draft ACI 440 I recommendations were found to correlate well with the measured results.

(4) The three different types of shear reinforcement had no practical effect on the static behaviour of the cantilever specimens in the bending/torsion moment ranges achieved in the tests. Nevertheless the use of a 0-90°-biaxial geogrid reinforcement (made of PVA fibres) proved to be advantageous giving a higher failure safety by increasing the ultimate load of the pole and allowing for a certain rest load carrying capacity after reaching the peak testing load.

(5) The ultimate capacity was roughly the same regardless of whether the fuse box was on the compressive or tensile flange. A slightly higher capacity was obtained when the fuse box opening was located on the neutral axis. Except where the PVA geogrid was used, all the poles failed due to tendon rupture.

(6) It is expected that the poles will provide a durable and cost-effective alternative to steel-prestressed poles for use in pedestrian and low speed traffic areas.

ACKNOWLEDGEMENTS

The authors would like to thank Dr. C.J. Burgoyne for his valuable advice regarding design and testing matters. The help of the director of SACAC AG, Mr. G. Bättig, of several SACAC engineers, and of the company's laboratory and production teams involved in the manufacture of the specimens, is greatly appreciated. We are also grateful to the technical staff of the Department of Engineering, University of Cambridge for their important contribution in the design of the experiments and carrying out the testing programme.

REFERENCES

- [1] Terrasi G. P., Bättig G., Brönnimann R., 2001: "High-strength spun concrete poles prestressed with CFRP", FRPRCS-5 "Non-Metallic Reinforcement for Concrete Structures", ISBN 07277-3009-6, University of Cambridge, England 16–18 Jul 2001, Ed. C. Burgoyne, pp. 1103-1112
- [2] CEN/TC 50 "Lighting columns and spigots": European Standard EN 40-1: 2000: Definitions and terms, European Committee for Standardization CEN, Brussels
- [3] CEN/TC 50 "Lighting columns and spigots": European Standard EN 40-2: 2000: General requirements and dimensions, European Committee for Standardization CEN, Brussels
- [4] CEN/TC 50 "Lighting columns and spigots": European Standards EN 40-3-1: 2000, EN40-3-2: 2000, prEN 40-3-3: 1999 (final draft): Design and verification, European Committee for Standardization CEN, Brussels
- [5] CEN/TC 50 "Lighting columns and spigots": European Standard EN 40-4: 2000: Specification for reinforced and prestressed concrete lighting columns, European Committee for Standardization CEN, Brussels
- [6] ACI 440 I "Guidelines for prestressing concrete structures with FRP tendons" Draft document, Feb 2003.

List of Tables

Table 1: Tendon material properties (based on 10 tensile tests)

Table 2: Summary of EN requirements and experimental results

Table 3: Predicted versus experimental load capacities (shaded boxes denote critical sections)

Table 1: Tendon material properties (based on 10 tensile tests)

fibre type	Tenax UTS
matrix	EP Bakelite Rütapox
nominal tendon diameter	4 mm
effective tendon diameter	3.95 mm (coated: 4.66 mm)
number of filaments per tendon	19 rovings at 12 K
fibre volume	67.8%
longitudinal tensile strength	2'292 N/mm ²
minimum strength (tensile test)	2'202 N/mm ²
mean longitudinal E modulus	161'000 N/mm ²
mean elongation at tensile rupture	1.45%
minimum elongation at rupture	1.37%

Table 2: Summary of EN requirements and experimental results






pole no.	Fuse opening location load direction ←	EN service test load (kN)	EN min. ultimate load (kN)	<i>Exper. deflect. at service test load (mm)</i>	<i>Exper. crack load (kN)</i>	<i>Exper. ultimate load (kN)</i>	<i>Exper. failure mode</i>
1	M _{+x} 	0.56	0.95	51.8	0.80	1.64	CFRP
2	M _y 	0.50	0.86	42.6	0.86	1.79	CFRP
3	M _{+x} 	0.56	0.95	52.0	0.95	1.89	HSSC
4	M _{-x} 	0.56	0.95	47.7	0.90	1.56	CFRP
5	M _{-x} 	0.56	0.95	51.2	1.0	1.64	CFRP

Table 3: Predicted versus experimental load capacities (shaded boxes denote critical sections)

Height from fixture (m)	Pole dia (mm)	P _o (MPa)	Pole 1 (M _{+x}) ultimate moment (failure load) fail mode		Pole 2 (M _y) ultimate moment (failure load) fail mode		Pole 3 (M _{+x}) ultimate moment (applied failure load) fail mode		Poles 4 & 5 (M _{-x}) ultimate moment (applied failure load) fail mode		
			Pred.	Exp.	Pred.	Exp.	Pred.	Exp.	Pred.	Exp. 4	Exp. 5
2.3	177	4.85	11.8 kNm (2.1 kN)		11.4 kNm (2.0 kN)		13.0 kNm (2.3 kN)		11.8 kNm (2.1 kN)		
1.8	182	5.57	9.2 kNm (1.5 kN) HSSC		11.9 kNm (1.9 kN)		9.6 kNm (1.6 kN) HSSC		10.9 kNm (1.8 kN) CFRP		
1.5	185	5.43	9.5 kNm (1.5 kN) HSSC		12.1 kNm (1.9 kN)		10.0 kNm (1.5 kN) HSSC	12.3 kNm (1.89 kN) HSSC	11.2 kNm (1.7 kN) CFRP		10.6 kNm (1.64 kN) CFRP
1.23										10.6 kNm (1.56 kN) CFRP	
1	190	4.43	12.6 kNm (1.8 kN)		12.1 kNm (1.7 kN)		14.5 kNm (2.1 kN)		12.6 kNm (1.8 kN)		
0.5	195	4.29	12.9 kNm (1.7 kN)		12.4 kNm (1.7 kN)		15.0 kNm (2.0 kN)		12.9 kNm (1.7 kN)		
0.28				12.6 kNm (1.64 kN) CFRP							
0	200	4.15	13.3 kNm (1.7 kN)		12.8 kNm (1.6 kN) CFRP	14.2 kNm (1.79 kN) CFRP <i>x=0.05 m</i>	15.5 kNm (1.9 kN)		13.3 kNm (1.7 kN)		

List of Figures

Figure 1: 27 m CFRP prestressed electricity pylon

Figure 2: Installed lighting column

Figure 3: Pole details (all dimensions in mm)

Figure 4: Experimental set-up

Figure 5: Plan view of displacement transducer locations (support conditions not shown)

Figure 6: Torsional behaviour

Figure 7: Crack pattern of pole 5 at reference load of 1.2 kN

Figure 8: Deflection profiles of pole 3 plotted at selected loads

Figure 9: Deflection of pole 3 during testing

Figure 10: Pole failure modes (a) tendon failure – pole 2 (b) steel buckling/concrete crushing – pole 3

Figure 11: Load vs. tip deflection behaviour of the poles 1-5 tested in cantilever bending/torsion



Figure 1



Figure 2

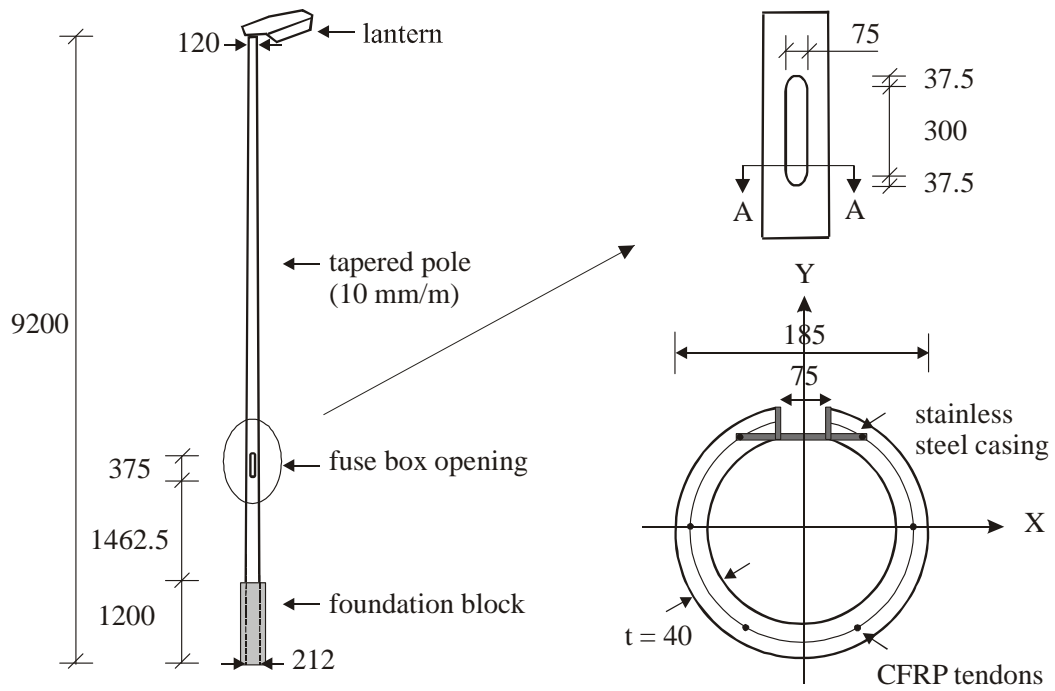


Figure 3

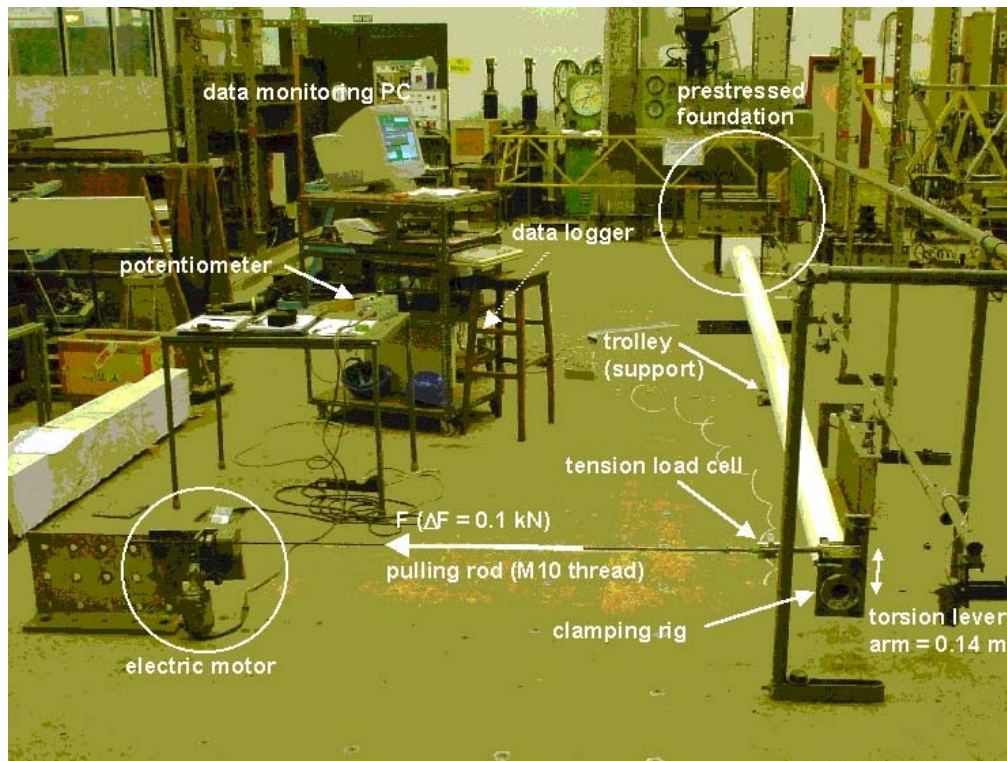


Figure 4

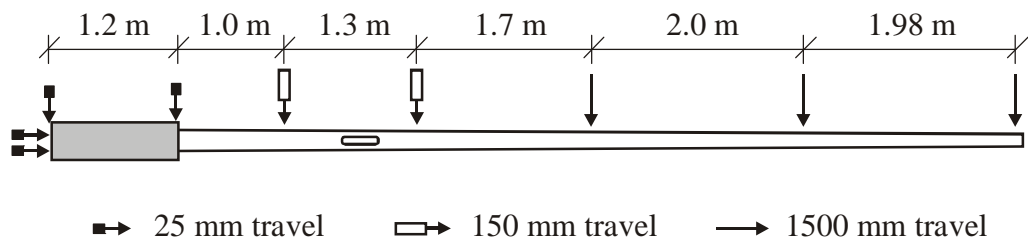


Figure 5

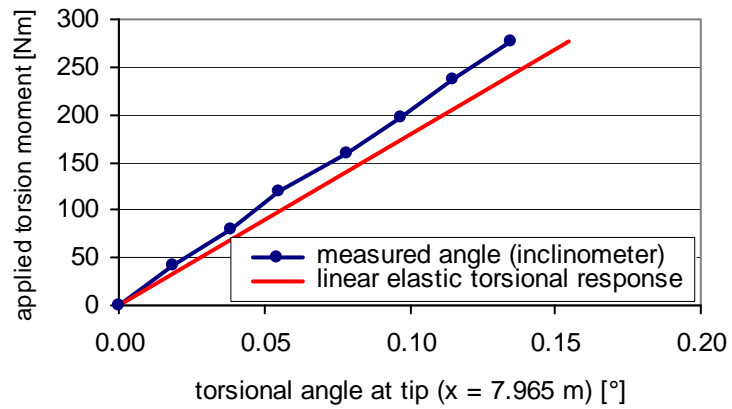


Figure 6

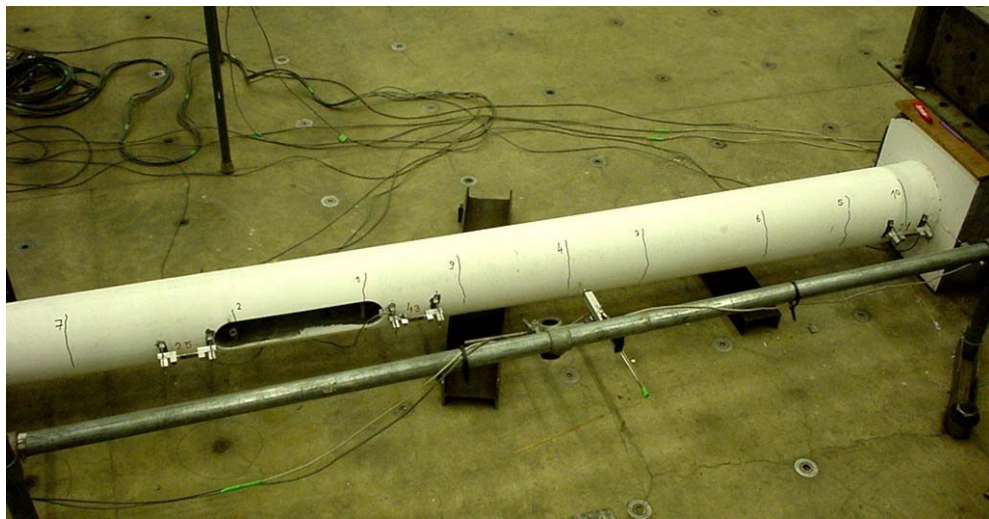


Figure 7

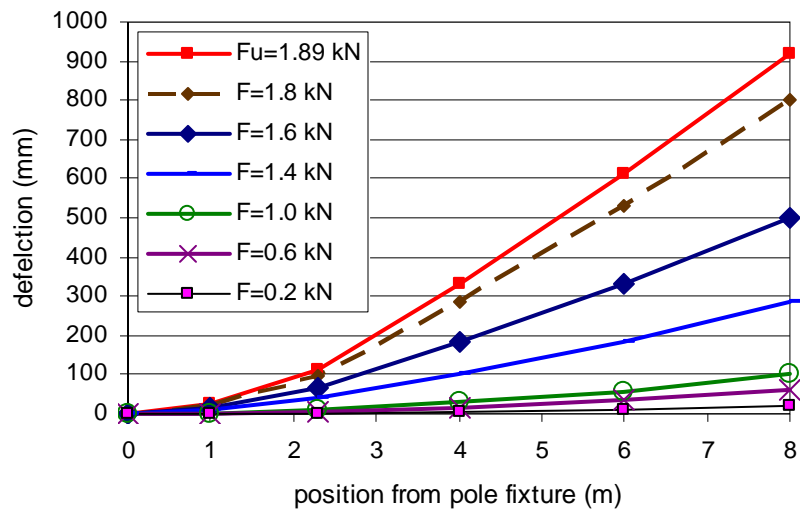


Figure 8

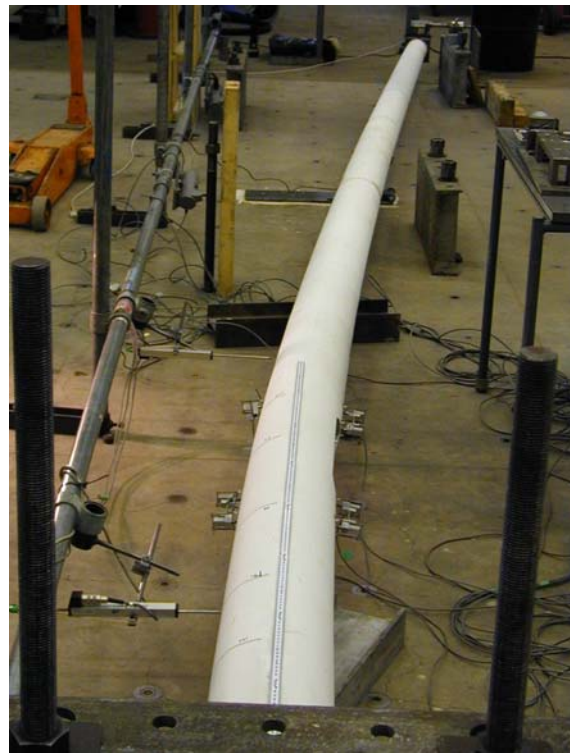


Figure 9



Figure 10 (a) (b)

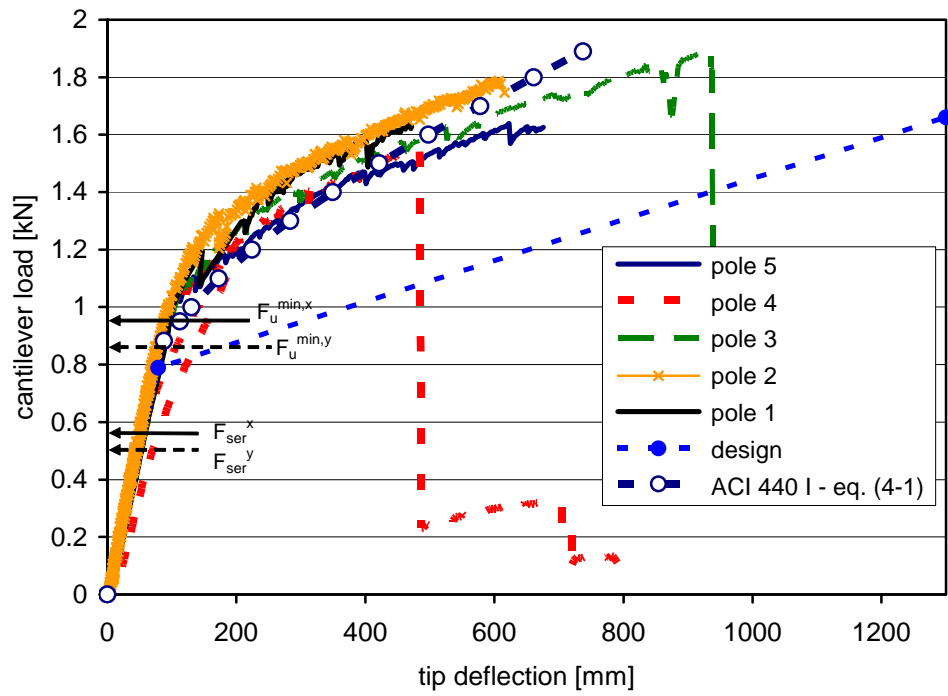


Figure 11